Electronic Properties of Carbon Nanotube-Nanoribbon Hybrids

李啟玄　　長庚大學通識中心
蘇萬生博士　台南科技大學通識中心
林明發教授　成功大學物理系

Outline

- Introduction
- Method
- Structual and Electronic Properties
- Conclusions

Introduction

Edge state in graphene ribbons: Nanometer size effect and edge shape dependence

Kyoko Nakada and Mitsutaka Fujita
Gene Dresselhaus and Mildred S. Dresselhaus
PRB 54, 1795[illegible]

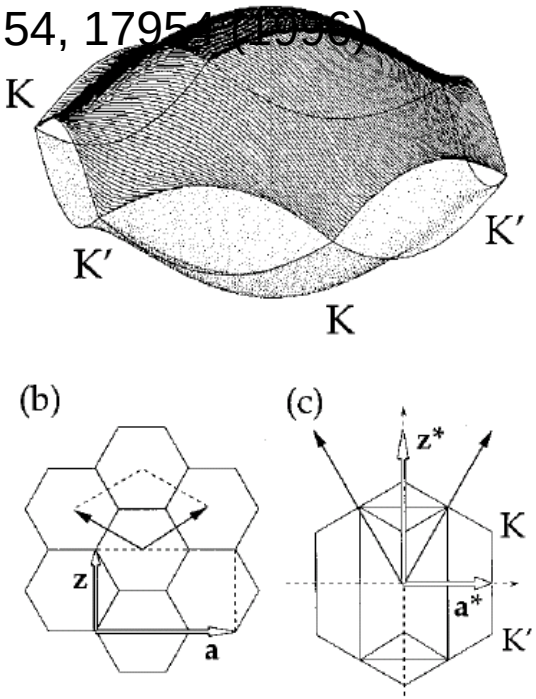

FIG. 2. Energy band structure (a) and unit cells in real space (b) and reciprocal space (c) of 2D graphite. The vectors **a** and **a*** (**z** and **z***) relate to armchair (zigzag) ribbons (see text) in (b) and (c). The valence and conduction bands make contact at the degeneracy point *K*.

Charge Carriers in Few-Layer Graphene Films

Sylvain Latil and Luc Henrard
PRL **97, 036803 (2006)**

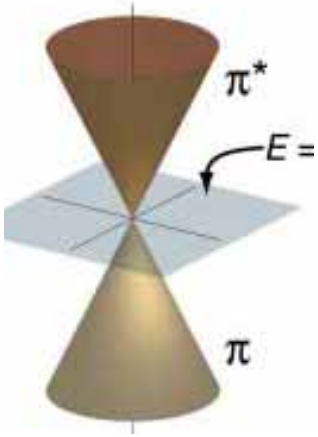

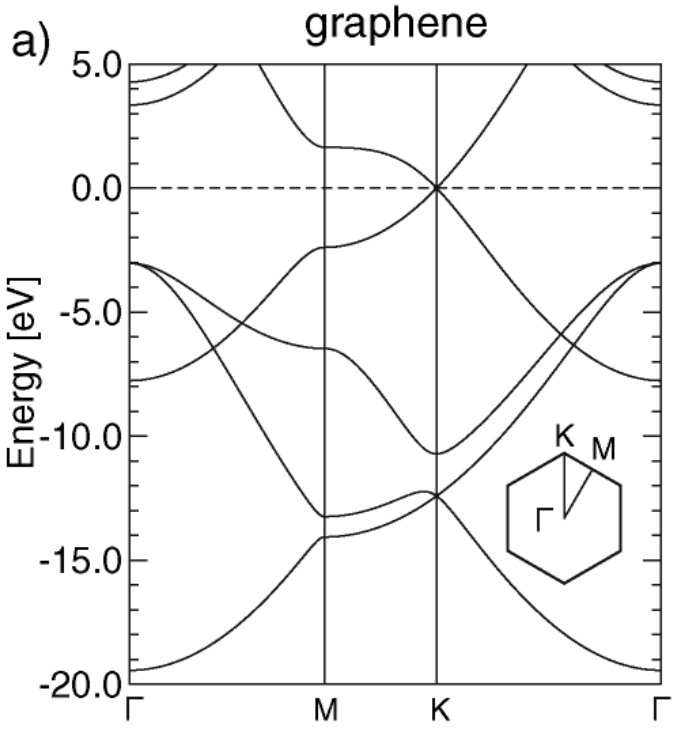

$C_h = na_1 + ma_2 = (n,m)$

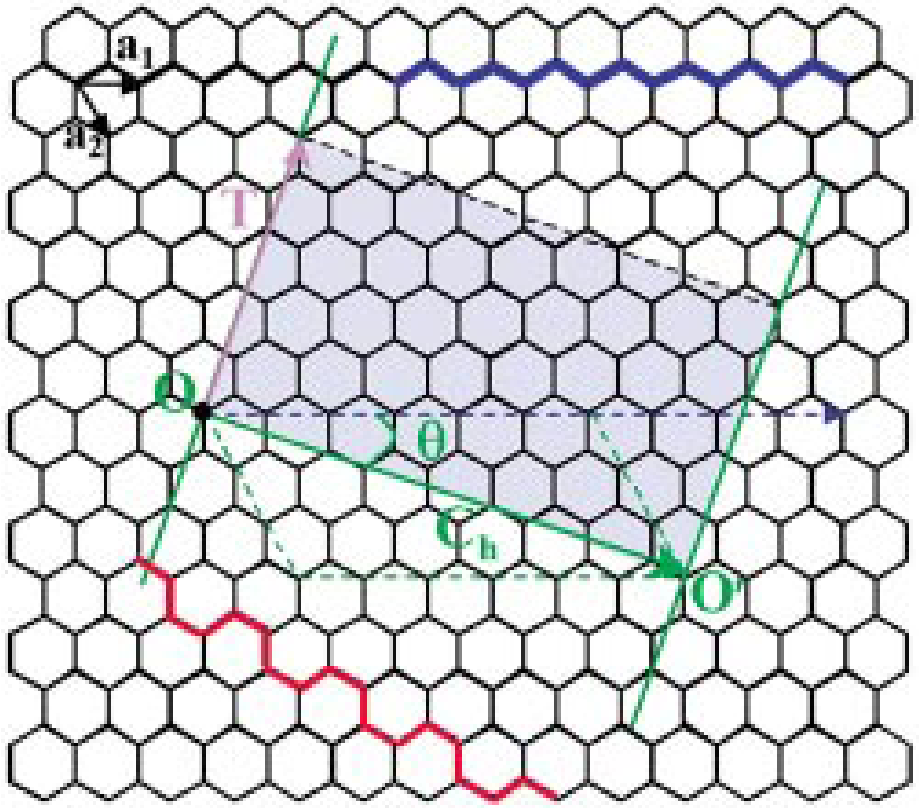

Zigzag (n,0)

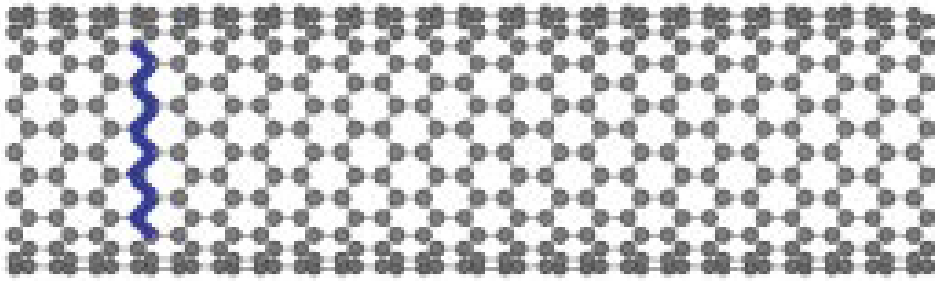

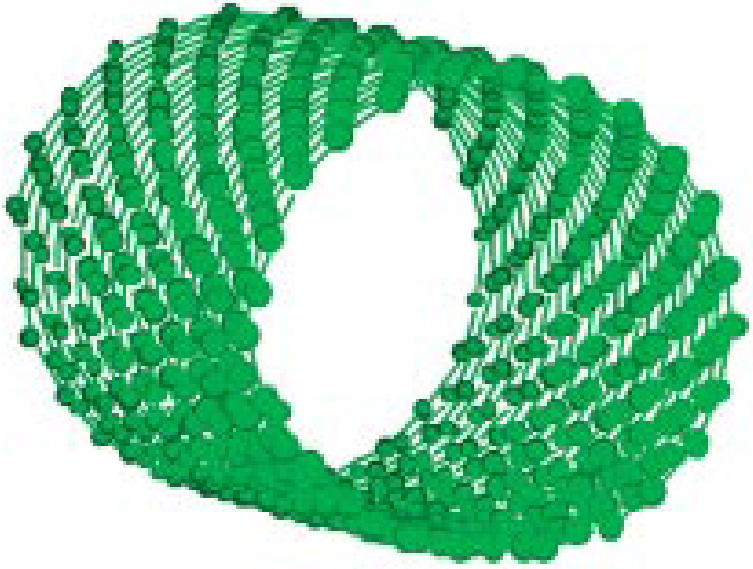

Armchair (n,n)

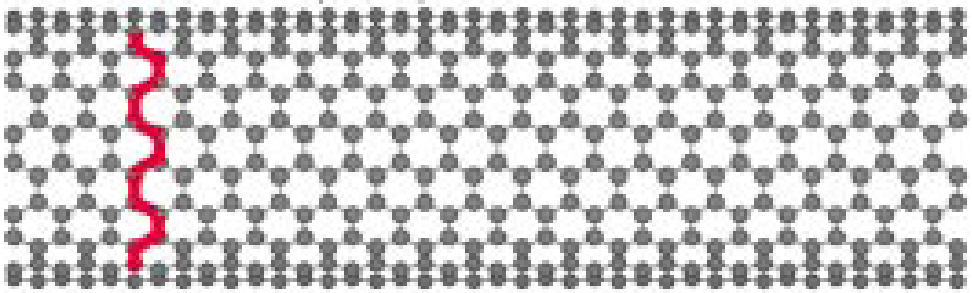

Chiral (n,m)

Annu. Rev. Phys. Chem. **53** :

$2p_z$ tight-binding model

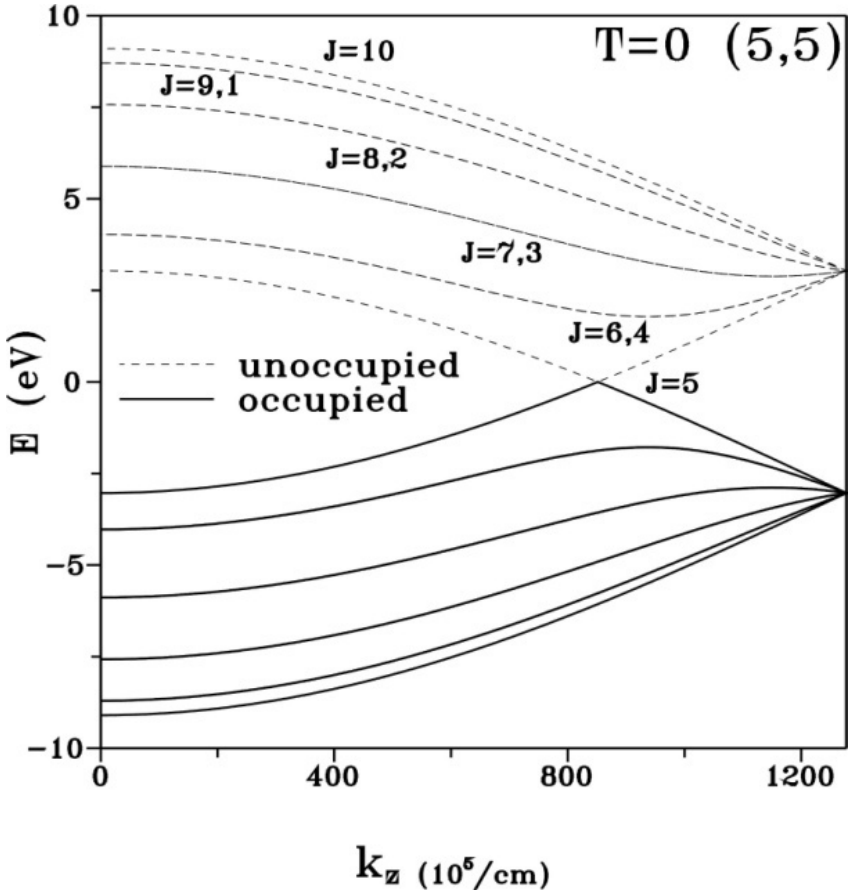

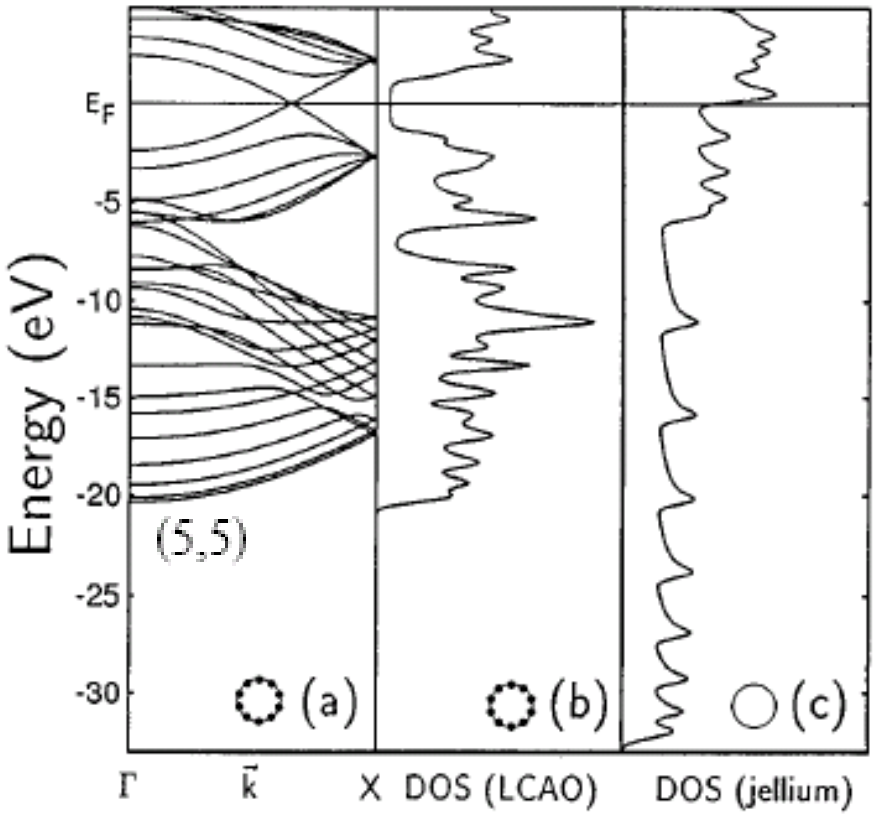

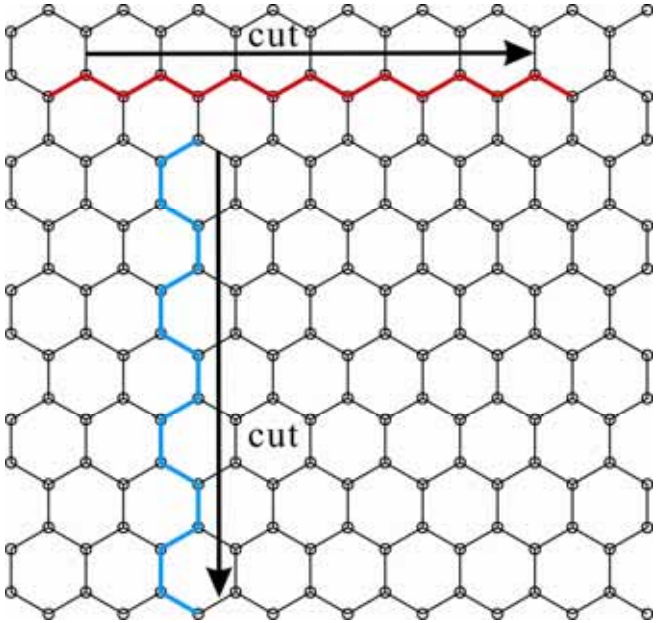

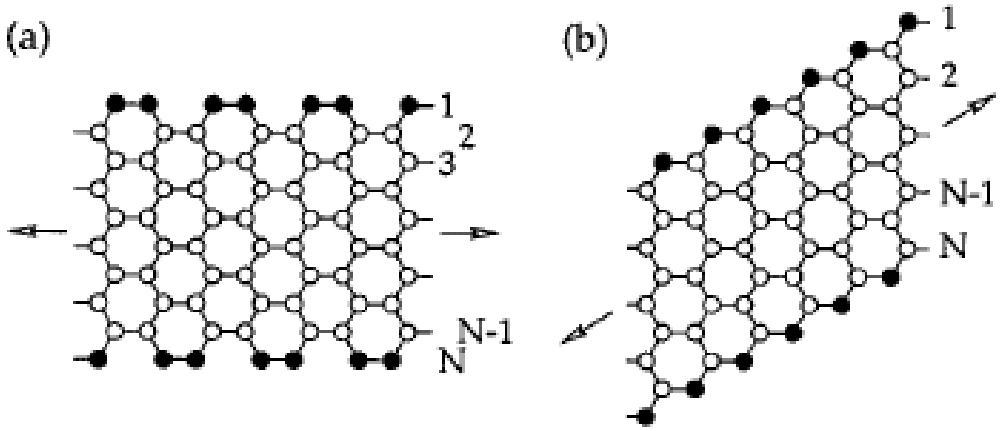

$2p_z$ tight-binding model

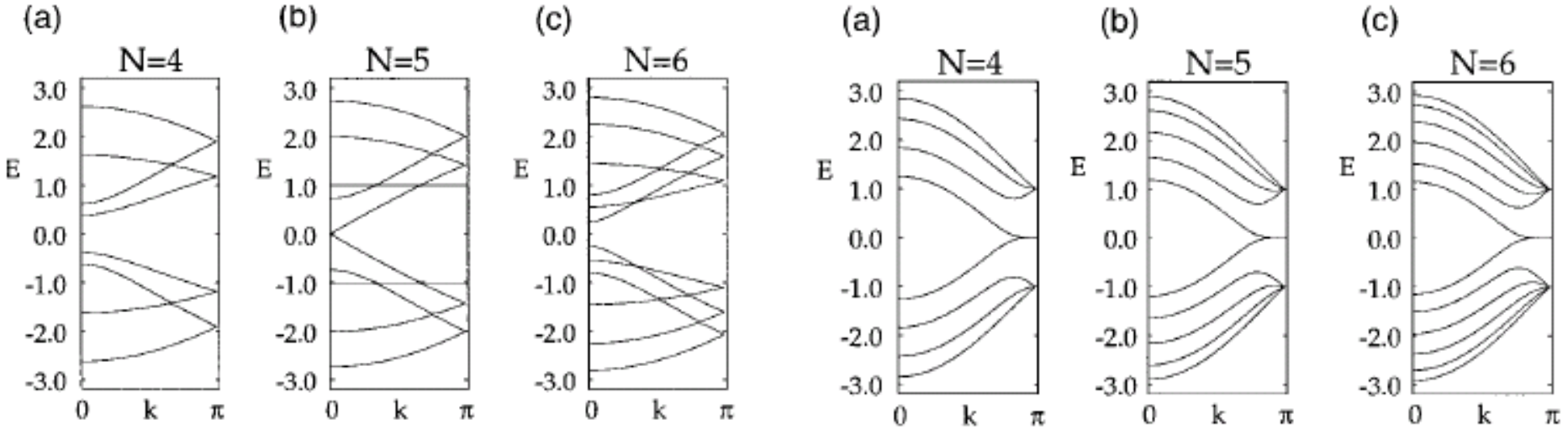

Armchair ribbon

zigzag ribbon

PRB 54 17954 (1996)

First-principles calculations for the zigzag graphene nanoribb

Band structures of zigzag ribbon with N=10

nonmagnetic (NM)

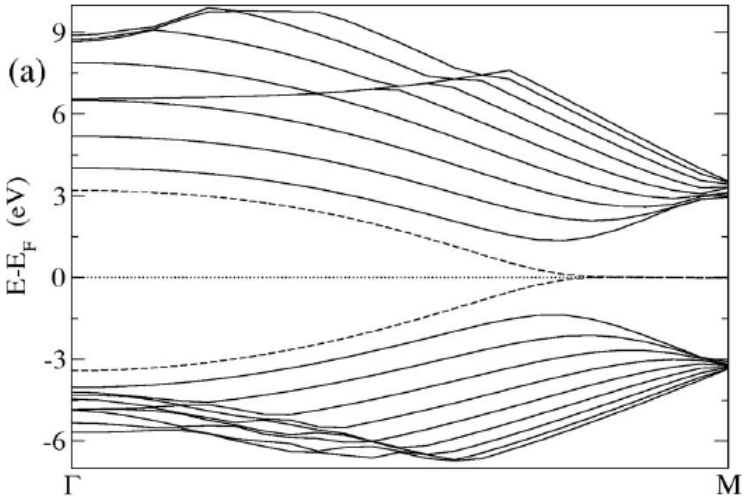

antiferromagnetic (AFM)

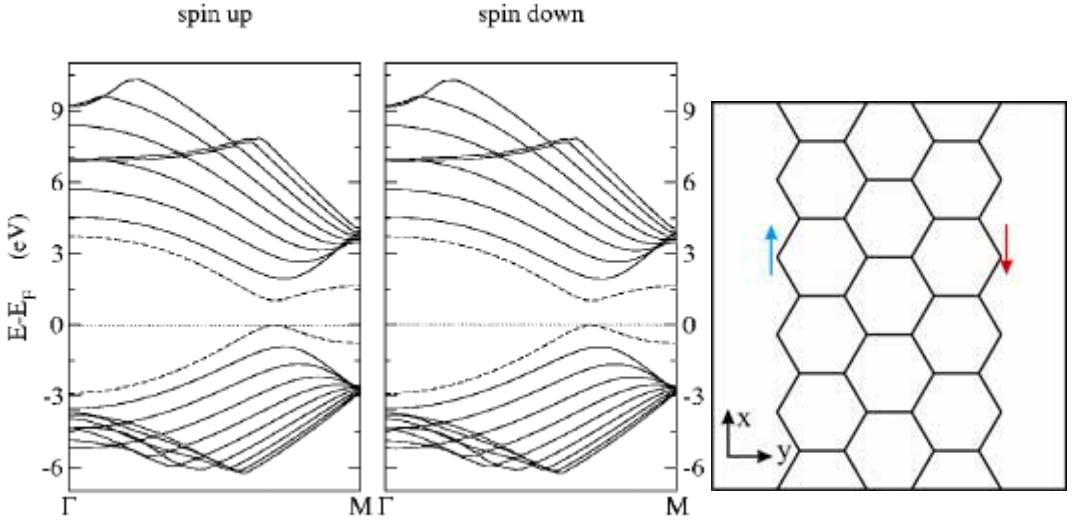

Both the AFM and FM configurations are found to have a total energy lower than the nonmagnetic state for all ribbon widths, indicating that spin polarization is a possible stabilization mechanism.
PRB 75, 064418 (2007)

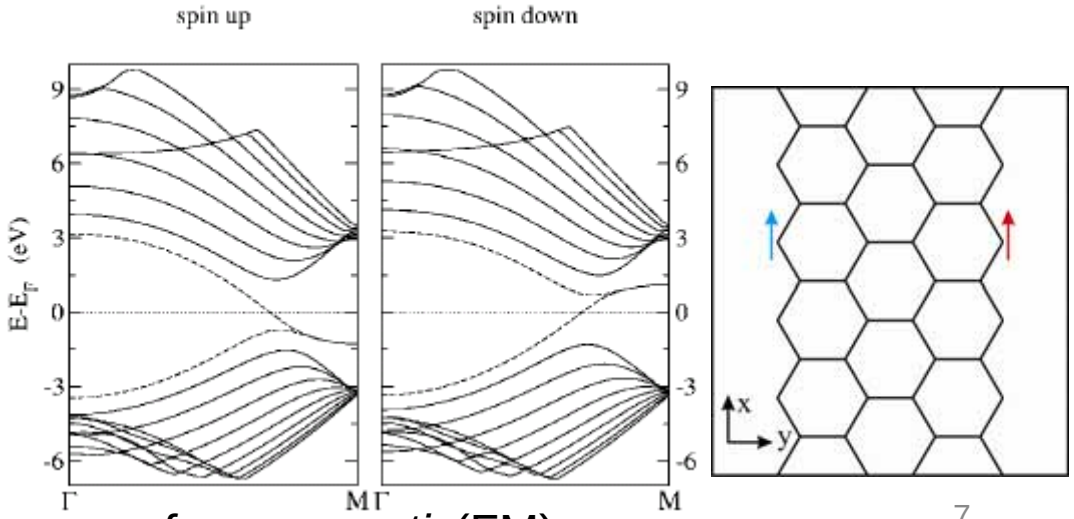

ferromagnetic(FM)

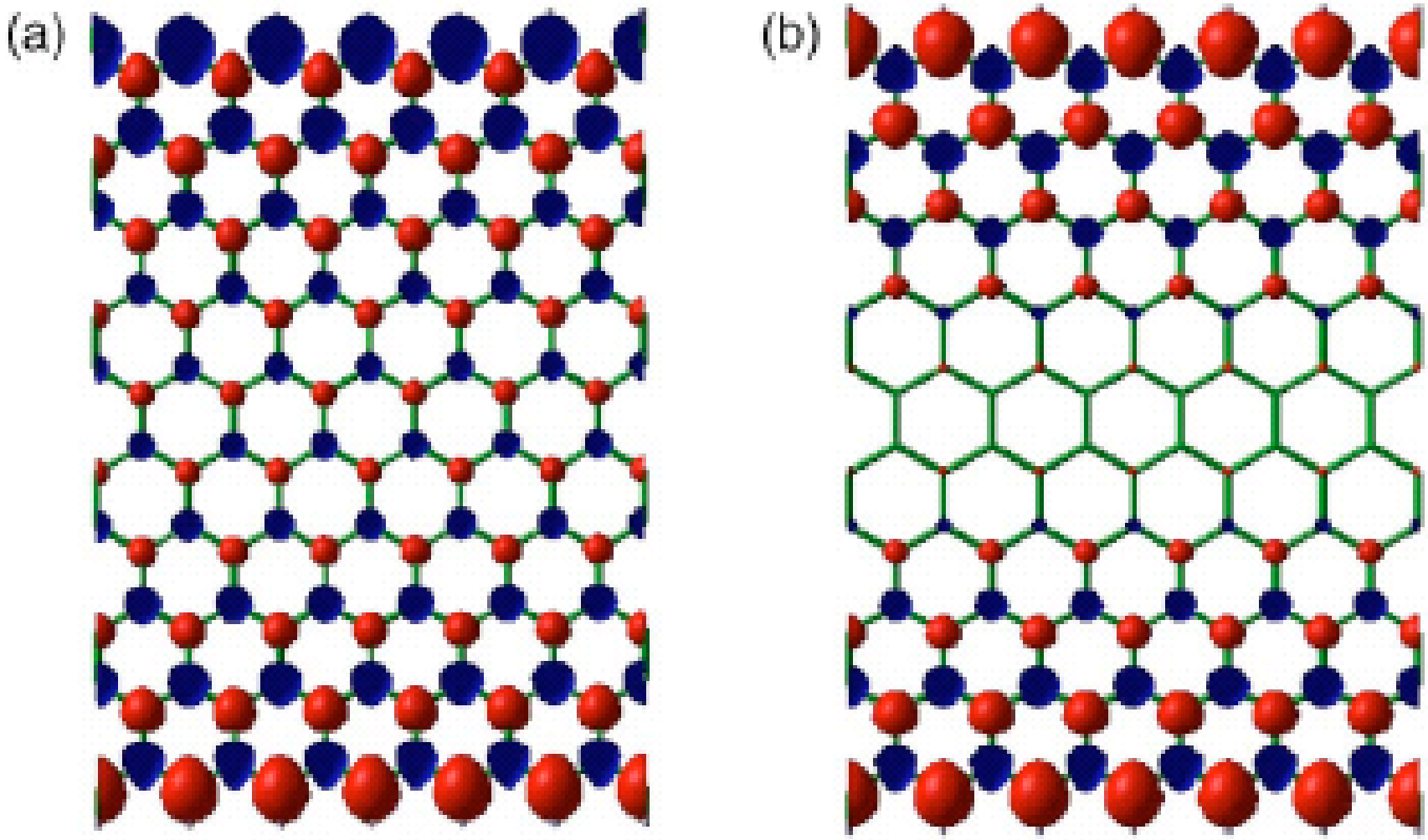
(a)
(b)

Narrow graphene nanoribbons from carbonnanotubes
Liying Jiao*, Li Zhang*, Xinran Wang, Georgi Diankov & Hongjie Dai
Nature **458**, 877 (2009)

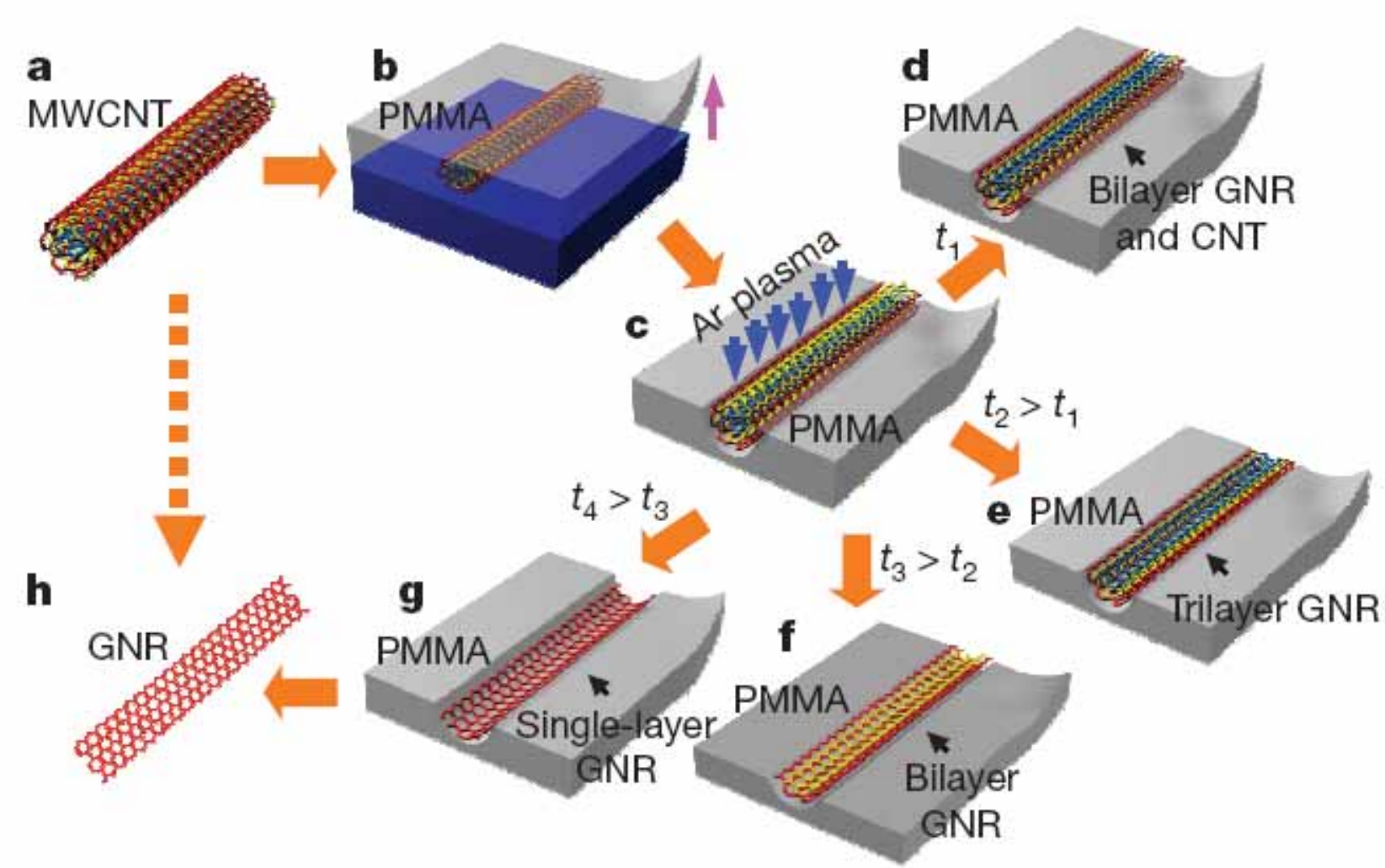

Method

- Package: Vienna Ab-Initio Simulation Package (VASP)

Schrödinger equation $H\psi_i = \varepsilon_i \psi_i$

$$H = \sum_{I=1}^{N} \frac{\vec{P}_I^2}{2M_I} + \sum_{i=1}^{N_e} \frac{\vec{p}_i^2}{2m} + \sum_{i>j} \frac{e^2}{|\vec{r}_i - \vec{r}_j|} + \sum_{I>J} \frac{Z_I Z_J e^2}{|\vec{R}_i - \vec{R}_J|} - \sum_{i,I} \frac{Z_I e^2}{|\vec{R}_I - \vec{r}_i|}$$

$$= T_N + T_e + V_{ee}(\vec{r}) + V_{NN}(\vec{R}) + V_{Ne}(\vec{r}, \vec{R})$$

LSDA

US

- Approximation: local spin density approximation (LSDA)
- Pseudopotential: ultrasoft pseudopotentials (US)
- The cutoff energy was set to 400 eV.
- The 80 ×1 ×1 Gamma-Pack grid was used to sample the first Brillouin-zone.
- All atoms were relaxed until the residual force < 0.01 eV/angstrom.

國家高速網路與計算中心
National Center for High-Performance Computing

- **Computing Nodes - 512 computing nodes.**
- **Each computing node consists of :**
- **CPU - Intel Woodcrest 3.0 Ghz Dual-Core processor Ｘ 2**
- **Memory - 16 GB PC2-5300 667MHz FBD 240-pin ECC DDR2-SDRAM**

Hostname : hpc
Model Name: IBM System p 9119-595

Hardware

CPU Architecture: SMP

Processor Type: PowerPC_POWER5
Number Of Processors: 64
Processor Clock Speed: 2302 MHz
CPU Type: 64-bit
Main Memory: 256 GB
Storage : 300GB 15K RPM SCSI Disk x 10

Geometrical Structures

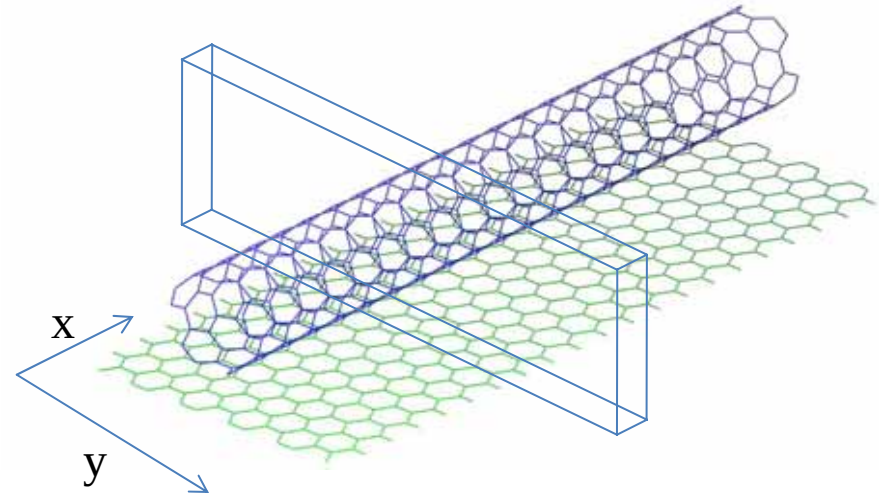

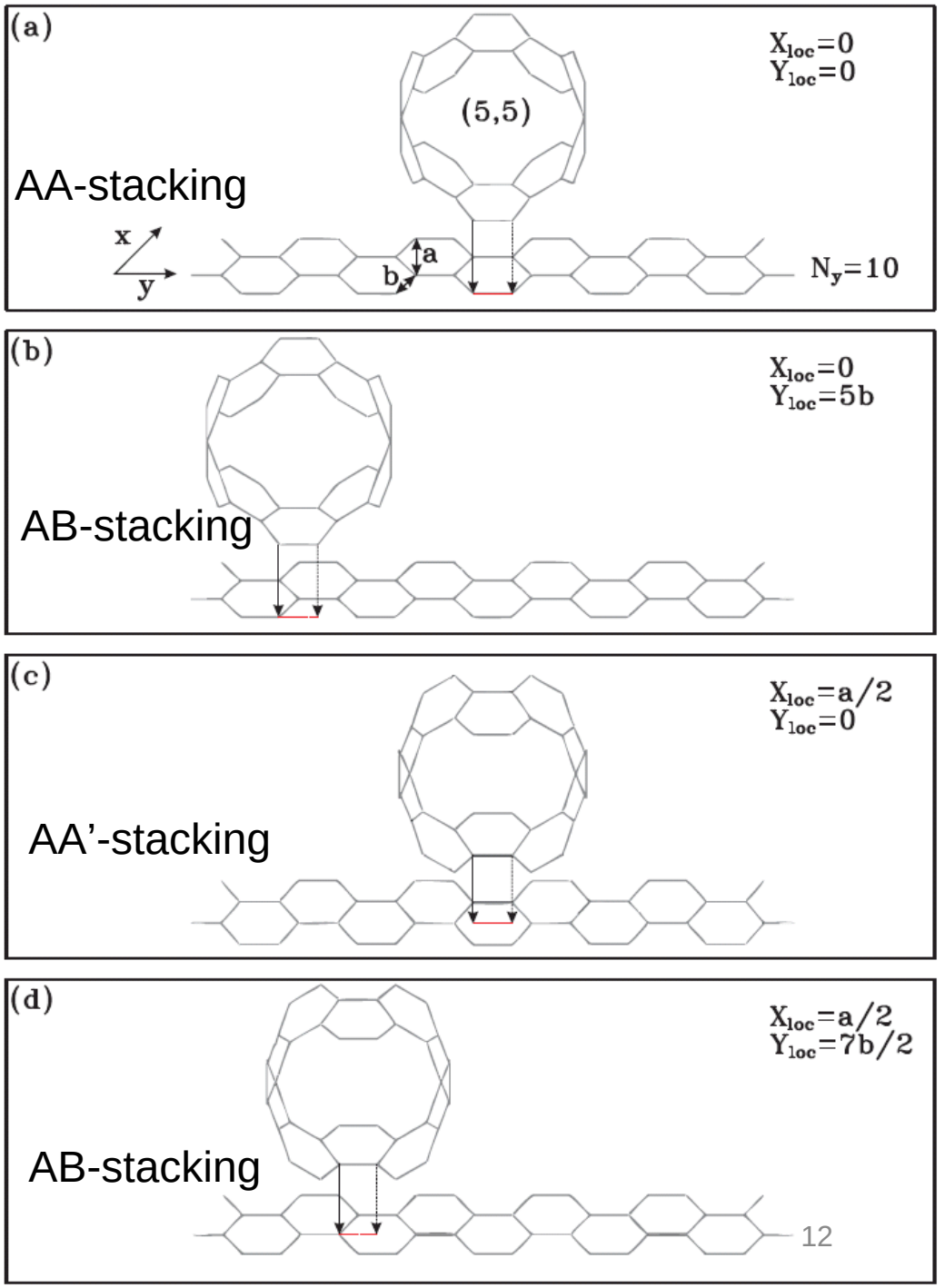

Structural properties

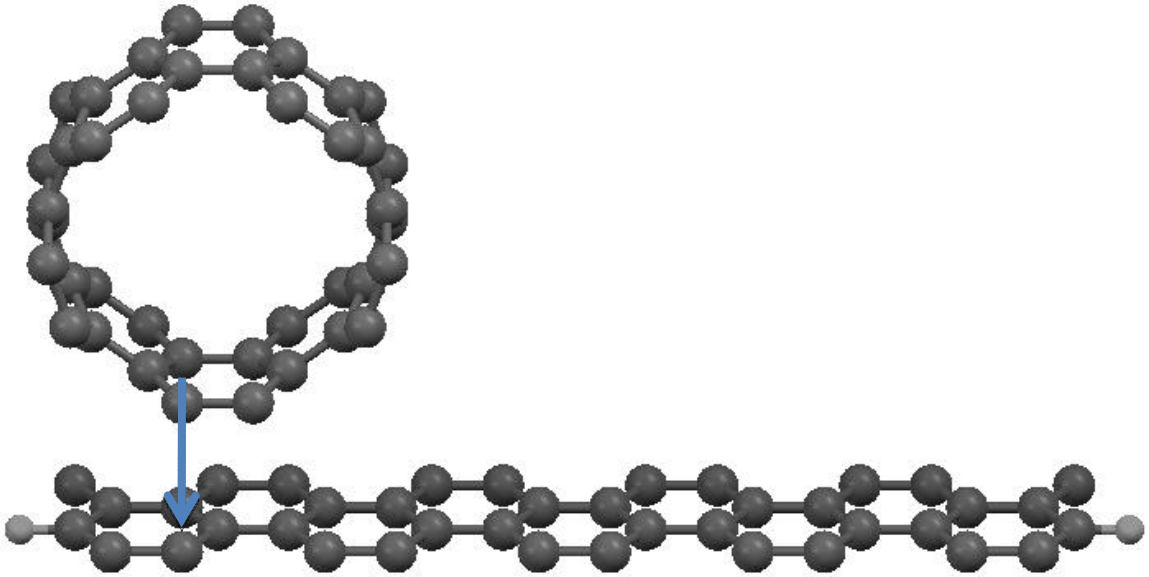

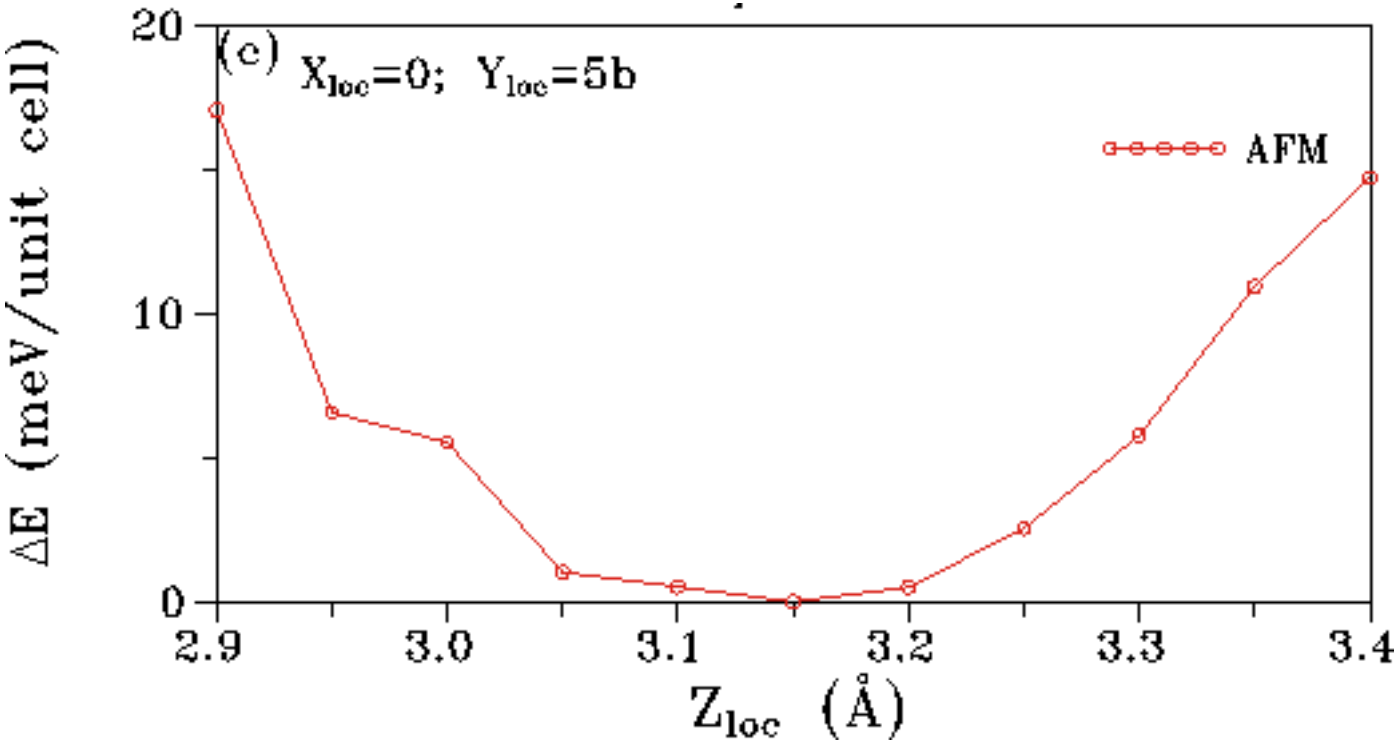

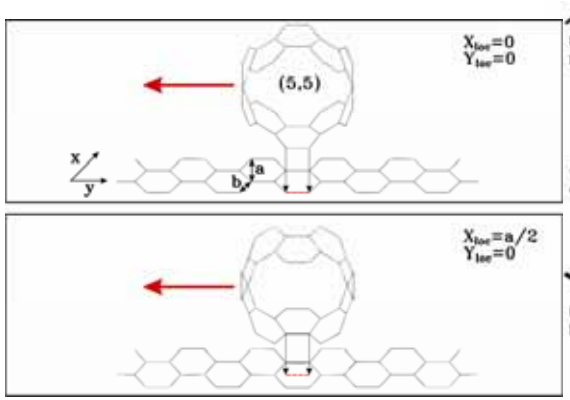

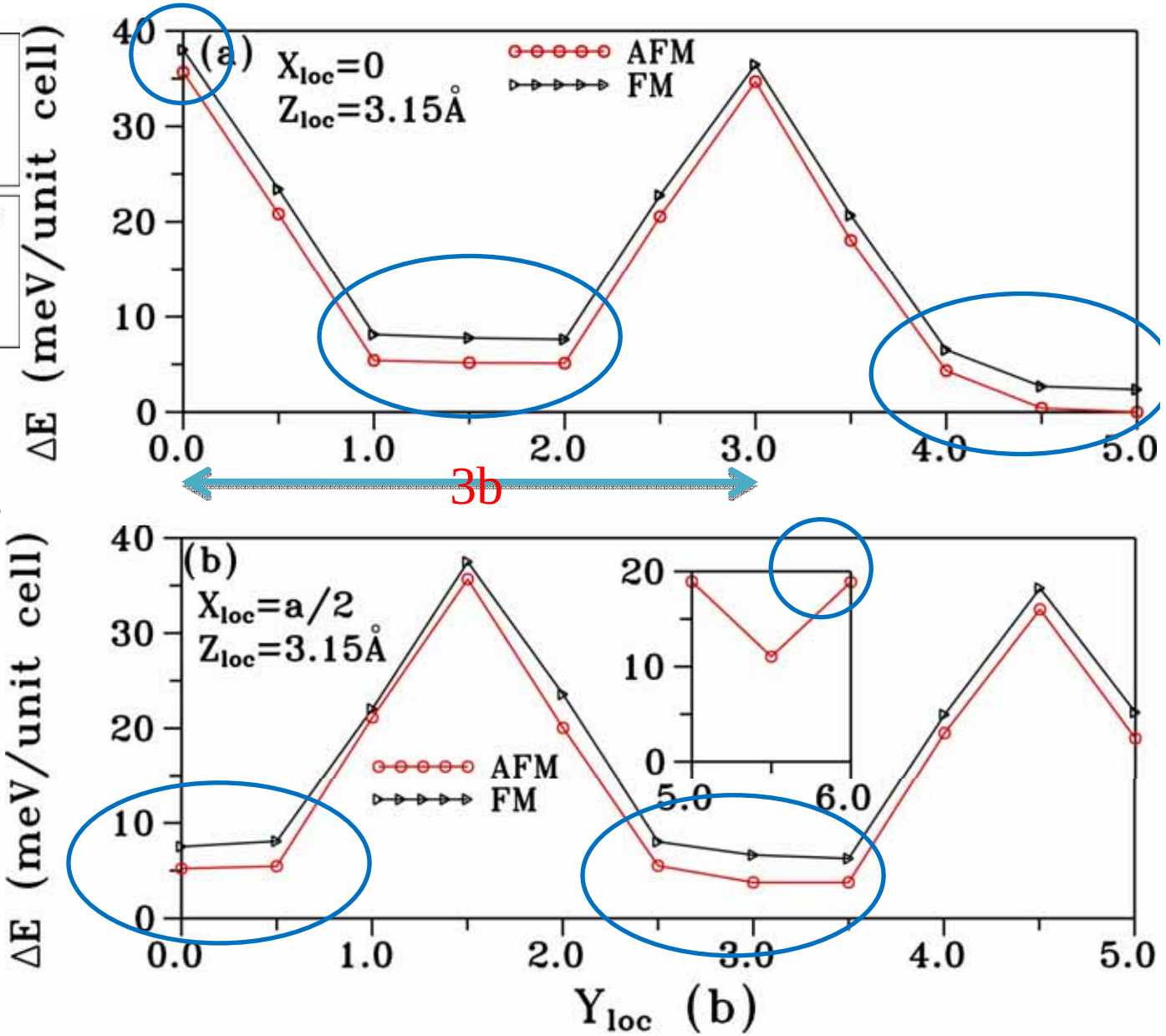

- The AFM configurations are always more stable than FM configuration.
- The AA-stacking is unstable.
- The AB- and AA'-stcking are the stable arrangement.

$X_{loc}=0$, $Y_{loc}=0$; AA-stacking

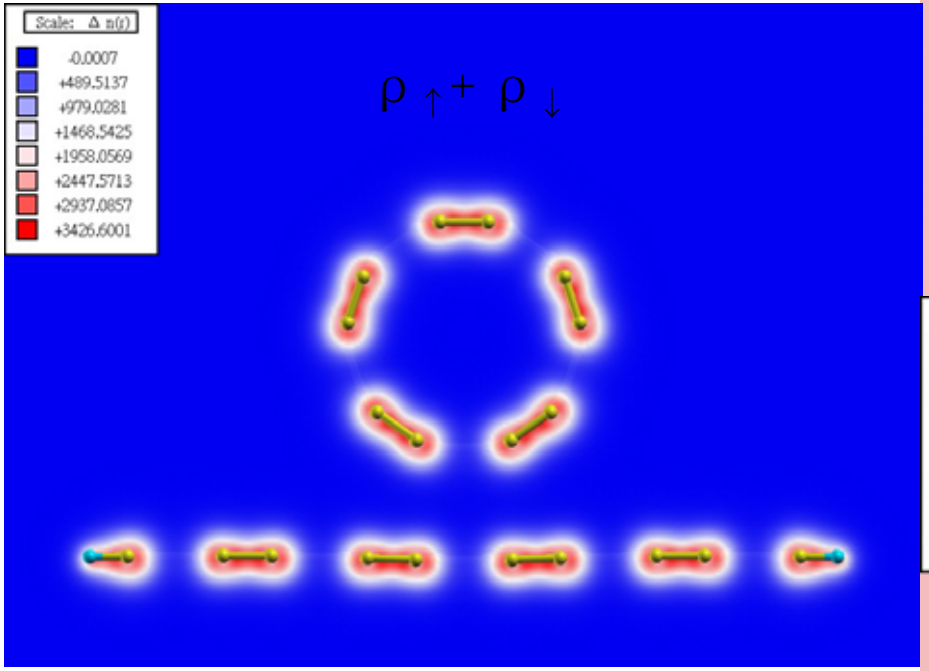

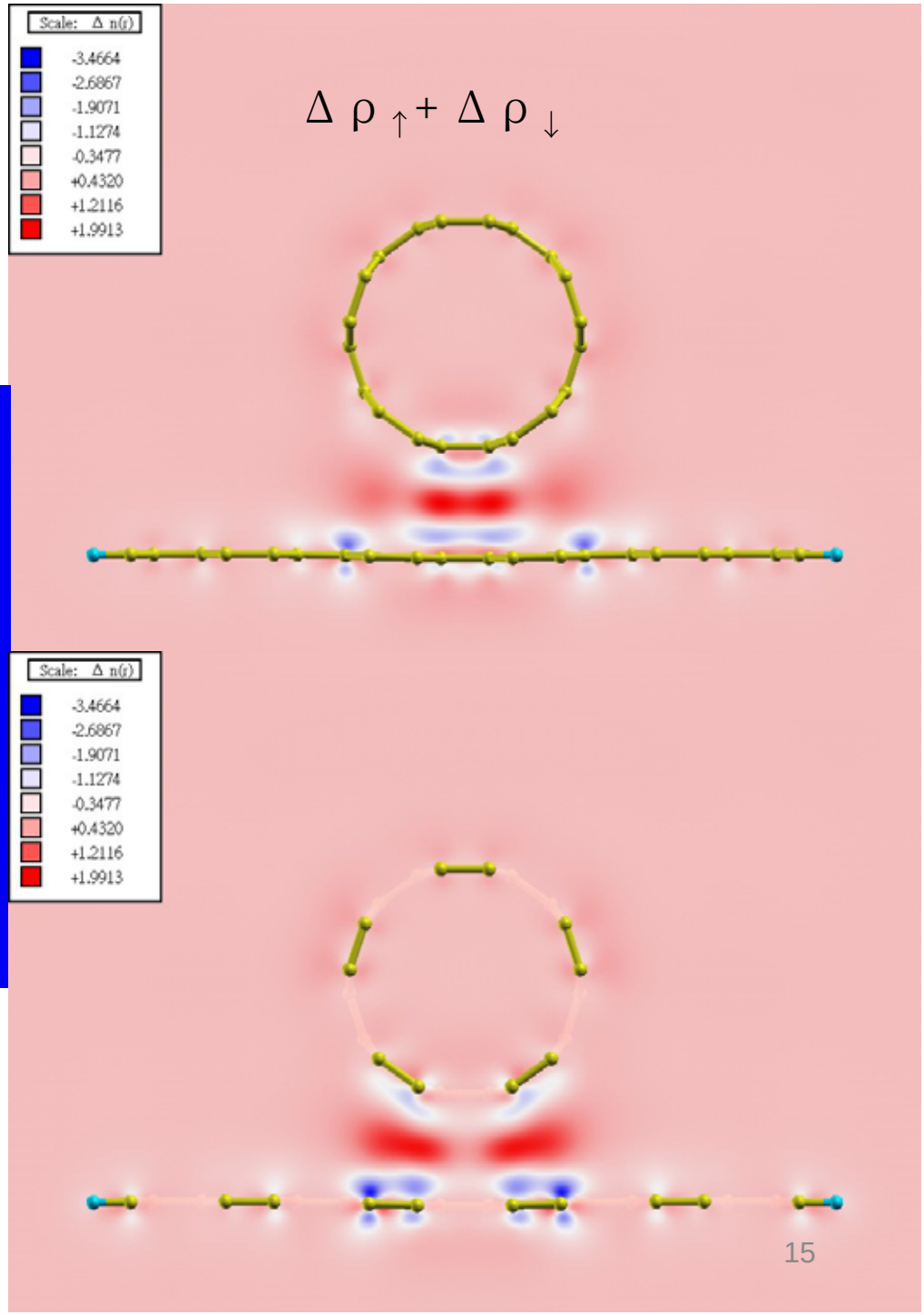

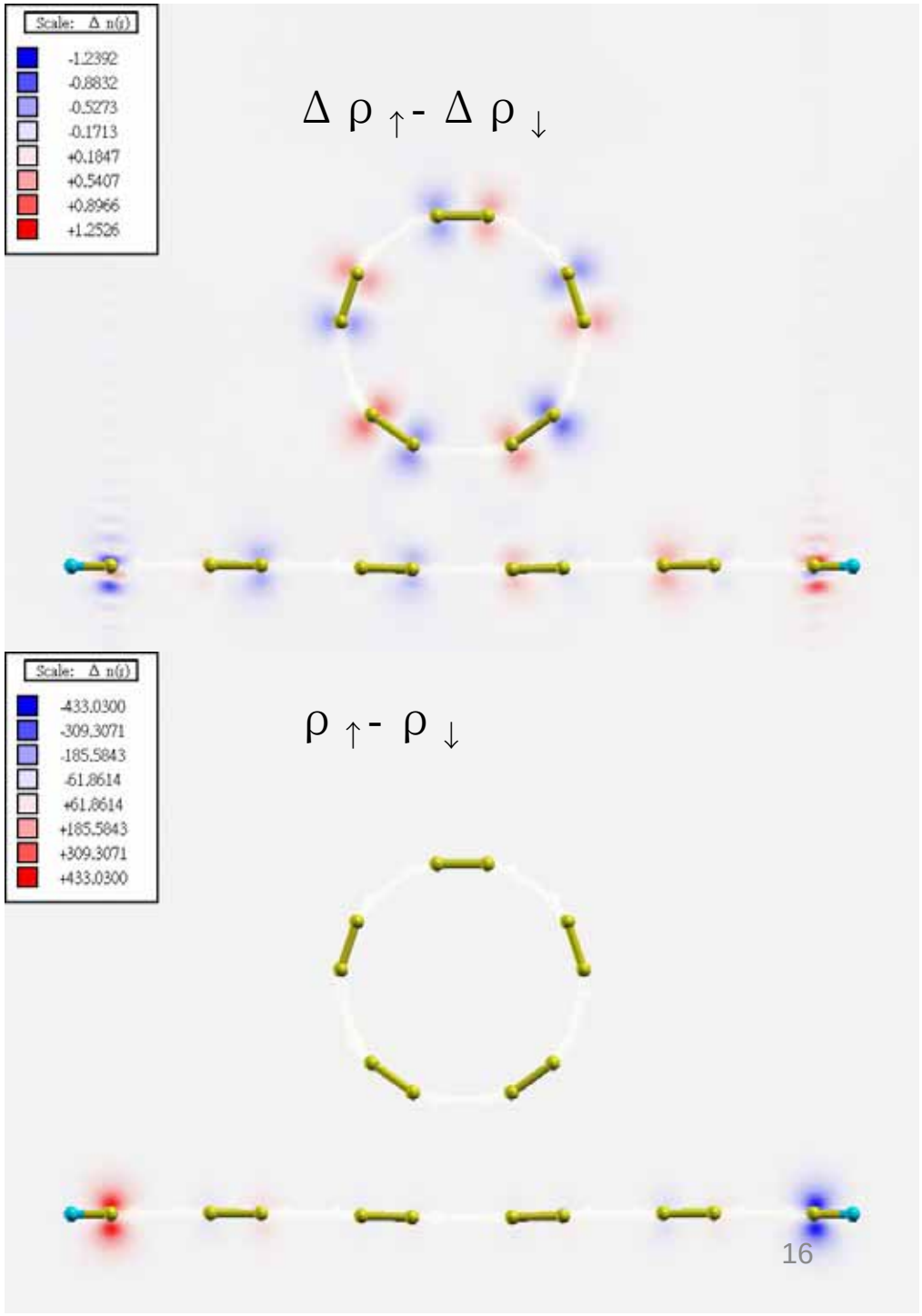
Scale: Δ n(r)
-1.2392
-0.8832
-0.5273
-0.1713
+0.1847
+0.5407
+0.8966
+1.2526
Δ ρ ↑- Δ ρ ↓
Scale: Δ n(r)
-433.0300
-309.3071
-185.5843
-61.8614
+61.8614
+185.5843
+309.3071
+433.0300
ρ ↑- ρ ↓

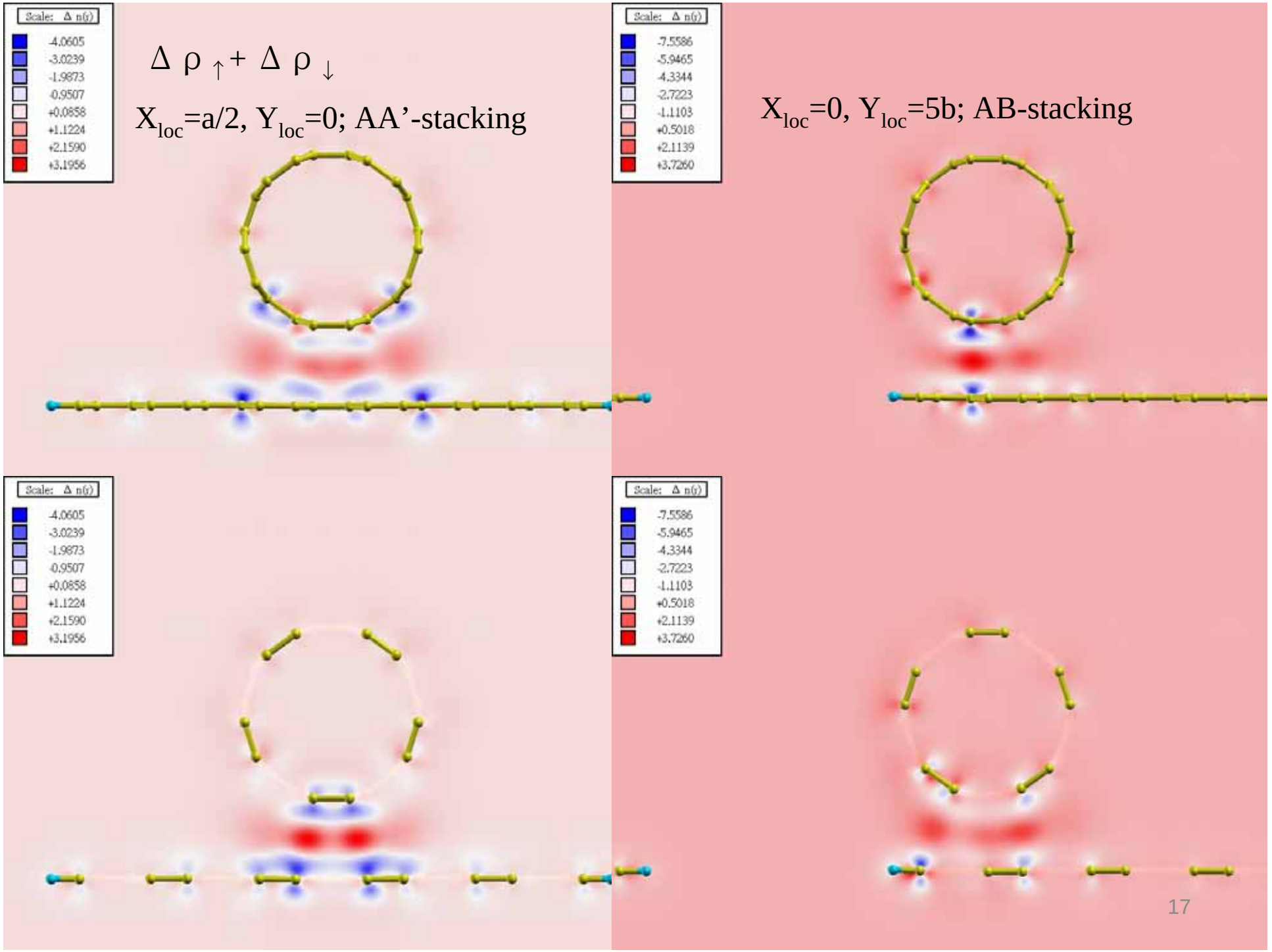
Scale: Δ n(r)
-4.0605
-3.0239
-1.9873
-0.9507
+0.0858
+1.1224
+2.1590
+3.1956
Δ ρ ↑+ Δ ρ ↓
X_loc=a/2, Y_loc=0; AA'-stacking
Scale: Δ n(r)
-7.5586
-5.9465
-4.3344
-2.7223
-1.1103
+0.5018
+2.1139
+3.7260
X_loc=0, Y_loc=5b; AB-stacking
Scale: Δ n(r)
-4.0605
-3.0239
-1.9873
-0.9507
+0.0858
+1.1224
+2.1590
+3.1956
Scale: Δ n(r)
-7.5586
-5.9465
-4.3344
-2.7223
-1.1103
+0.5018
+2.1139
+3.7260

Electronic properties

●A gap and new band-edge states emerge after considering the interlayer interactions.

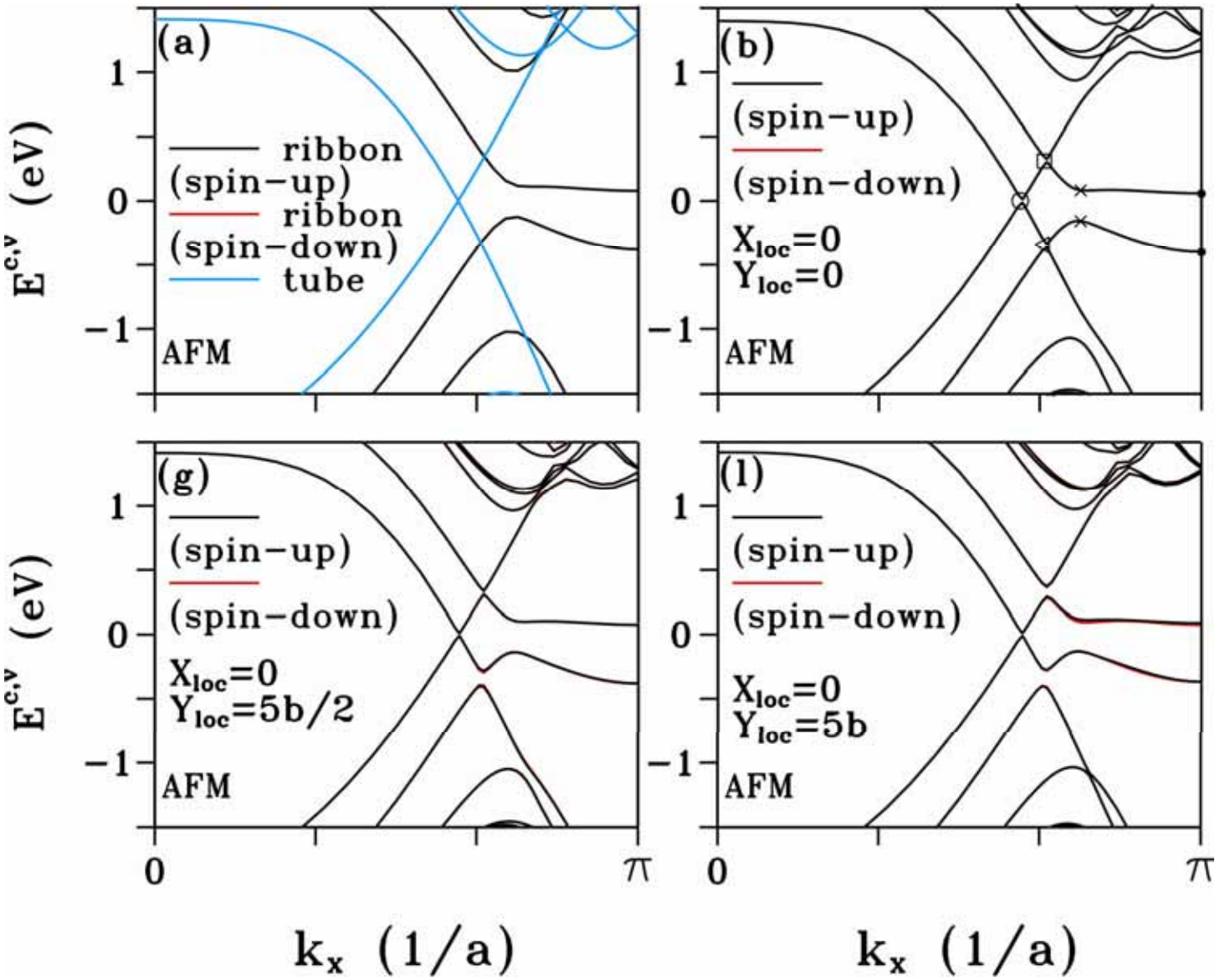

- The spin-up and spin-down states still cross at E_F.
- The shift of the tube breaks the degeneracy of states at $k_x = \pi/a$.

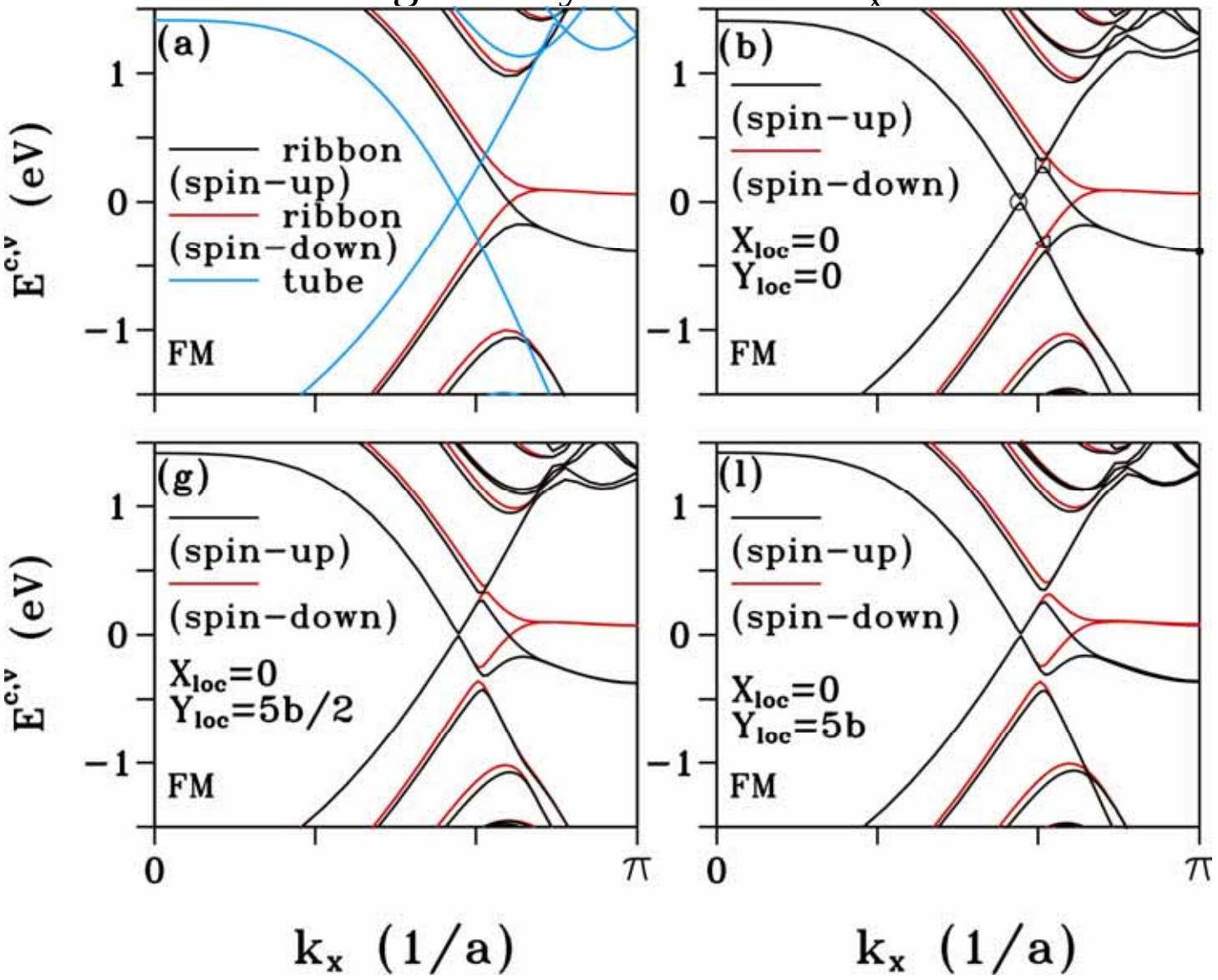

- The smaller gaps occur at the AA- and AA'-stacking.

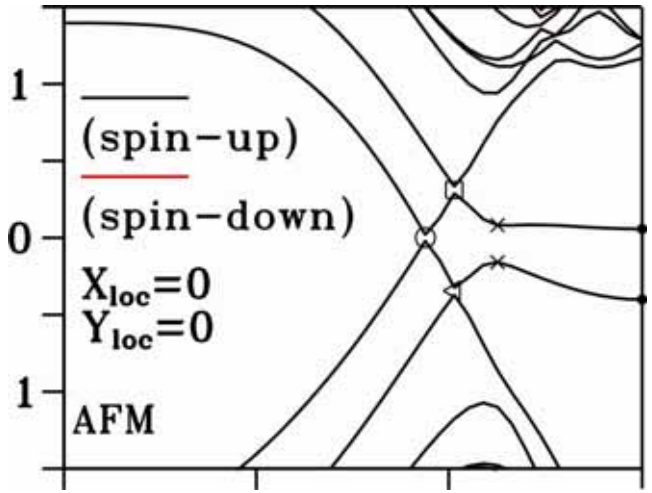

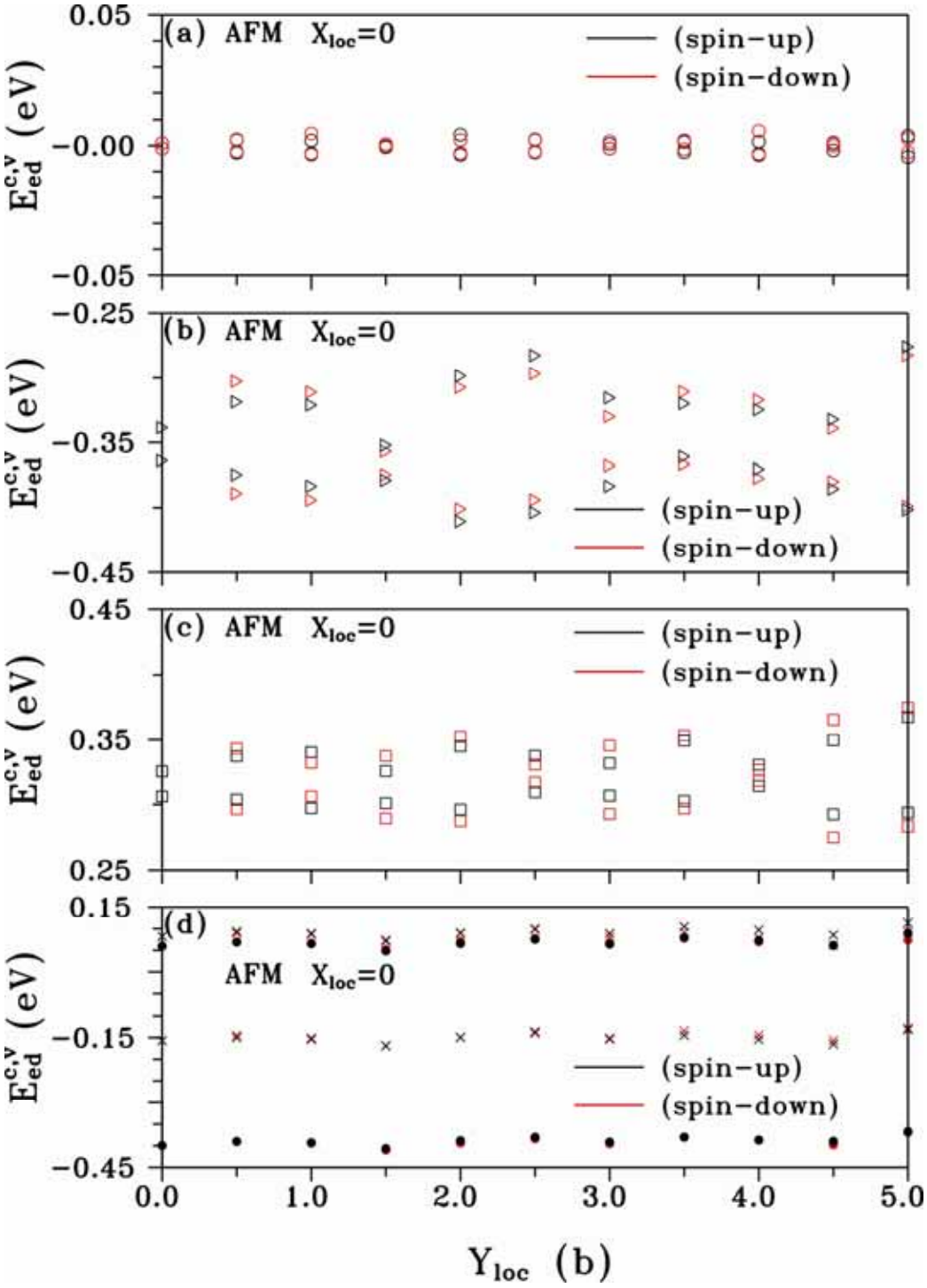

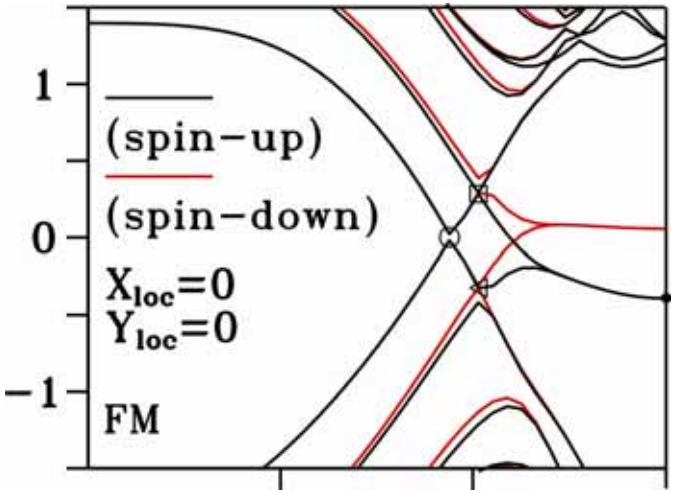
1
0
−1
(spin−up)
(spin−down)
X_loc=0
Y_loc=0
FM

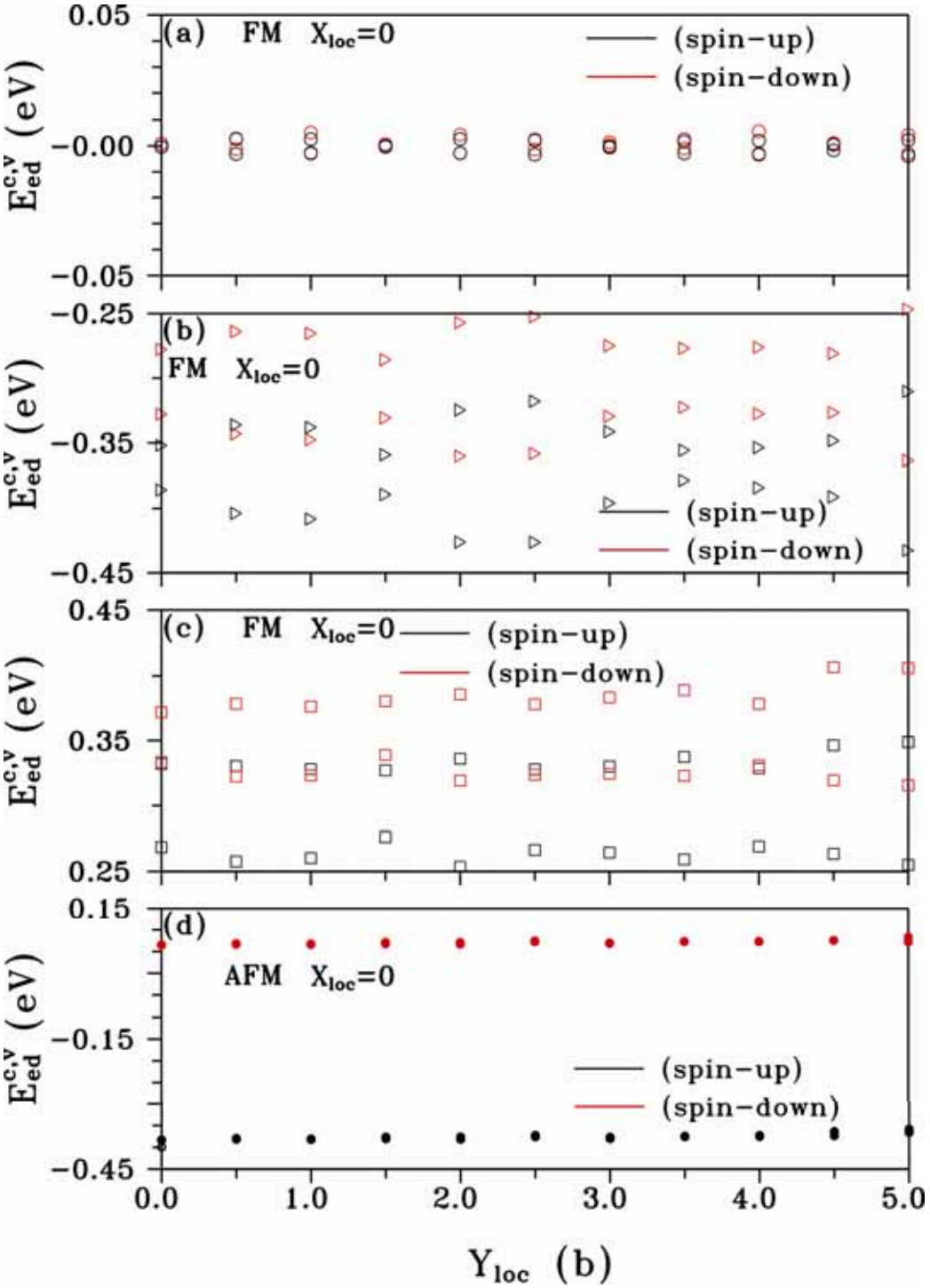
(a) FM X_loc=0
(spin−up)
(spin−down)
(b) FM X_loc=0
(spin−up)
(spin−down)
(c) FM X_loc=0
(spin−up)
(spin−down)
(d) AFM X_loc=0
(spin−up)
(spin−down)
E^{c,v}_{ed} (eV)
0.05
−0.00
−0.05
−0.25
−0.35
−0.45
0.45
0.35
0.25
0.15
−0.15
−0.45
0.0
1.0
2.0
3.0
4.0
5.0
Y_loc (b)

Conclusion

- The tube approaching the border of the ribbon and forming the AB-stacked arrangement is most stable in this hybrids.

- The energy gap in the antiferromagnetic configuration stems from the linear bands of the armchair carbon nanotube and strongly depends on the nanotube location.

- The nanotube lying on the zigzag nanoribbon would break the degeneracy of the partial flat bands originating mainly from the ribbon. The separation would enlarge as the tube shifts toward the ribbon edge.

Van der Waals binding energies in graphitic structures

PHYSICAL REVIEW B, VOLUME 65, 125404

TABLE I. Binding energy of a fullerene molecule interacting with other graphitic structures.

Interacting with	Reference	Binding energy (eV/molecule)	No. of relevant interactions
fullerene	2	0.277	364
on top of a (10,10) tube	4	0.537	732
graphite	11	0.968	1001
mouth of a (10,10) tube	4	1.63	2270
inside a (10,10) tube	4	3.26	4112
at a spherical cap	4	4.40	5416

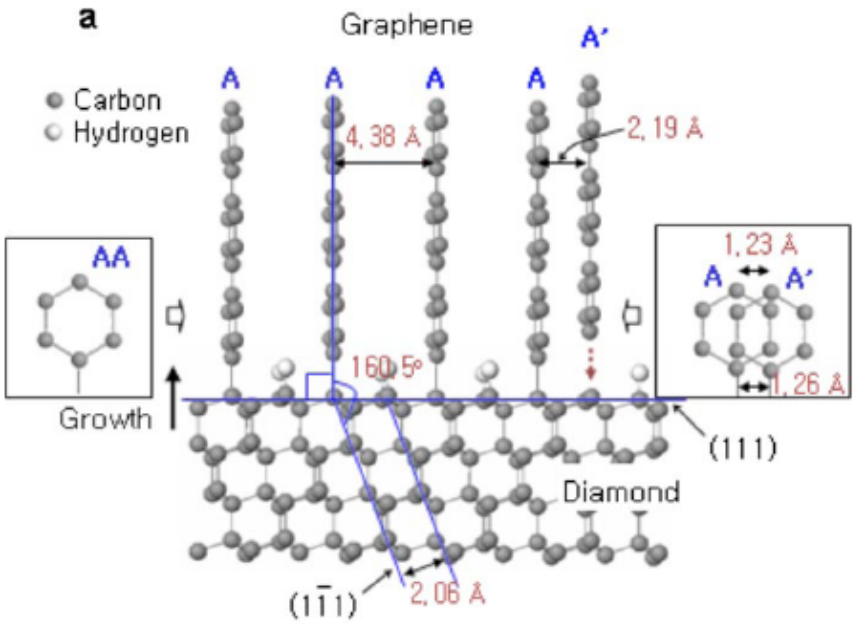

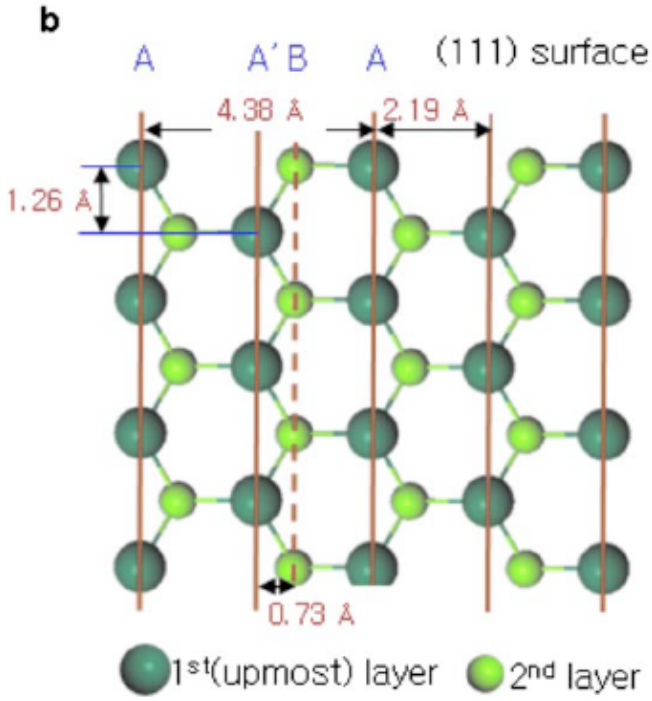

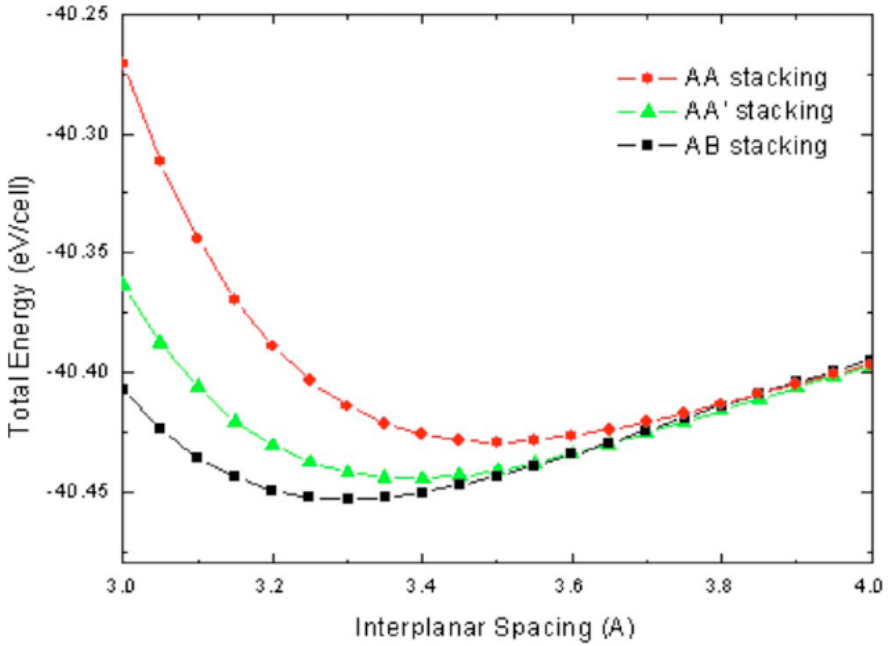

FIG. 3. (Color online) Potential energy surfaces of the *AB*, *AA′*, and *AA* graphites.

	AB stacking	*AA′* stacking	*AA* stacking
Calculated (0 K)	3.30	3.38	3.50
Measured (~300 K)	3.35 (Ref. 21)	3.43 (This work)	3.55 (This work)

J. Chem. Phys. **129, 234709 2008**